NIH Public Access
Author Manuscript
Dent Mater. Author manuscript; available in PMC 2013 October 01.

Published in final edited form as:
Dent Mater. 2012 October ; 28(10): 1059–1070. doi:10.1016/j.dental.2012.06.009.

Calcium phosphate cement with biofunctional agents and stem cell seeding for dental and craniofacial bone repair

WahWah Thein-Han[1], **Jun Liu**[1], and **Hockin H. K. Xu**[1,2,3,4]

[1]Biomaterials & Tissue Engineering Division, Department of Endodontics, Prosthodontics and Operative Dentistry, University of Maryland Dental School, Baltimore, MD 21201, USA

[2]Center for Stem Cell Biology & Regenerative Medicine, University of Maryland School of Medicine, Baltimore, MD 21201, USA

[3]University of Maryland Marlene and Stewart Greenebaum Cancer Center, University of Maryland School of Medicine, Baltimore, MD 21201, USA

[4]Department of Mechanical Engineering, University of Maryland, Baltimore County, MD 21250, USA

Abstract

Objectives—Calcium phosphate cement (CPC) can be injected to harden *in situ* and is promising for dental and craniofacial applications. However, human stem cell attachment to CPC is relatively poor. The objectives of this study were to incorporate biofunctional agents into CPC, and to investigate human umbilical cord mesenchymal stem cell (hUCMSC) seeding on biofunctionalized CPC for osteogenic differentiation for the first time.

Methods—Five types of biofunctional agents were used: RGD (Arg-Gly-Asp) peptides, human fibronectin (Fn), fibronectin-like engineered polymer protein (FEPP), extracellular matrix Geltrex, and human platelet concentrate. Five biofunctionalized CPC scaffolds were fabricated: CPC-RGD, CPC-Fn, CPC-FEPP, CPC-Geltrex, and CPC-Platelets. The hUCMSC attachment, proliferation, osteogenic differentiation and mineral synthesis were measured.

Results—The hUCMSCs on biofunctionalized CPCs had much better cell attachment, proliferation, actin fiber expression, osteogenic differentiation and mineral synthesis, compared to the traditional CPC control. Cell proliferation was increased by an order of magnitude via incorporation of biofunctional agents in CPC ($p < 0.05$). Mineral synthesis on biofunctionalized CPCs were 3-5 folds of those of control ($p < 0.05$). hUCMSCs differentiated with high alkaline phosphatase, Runx2, osteocalcin, and collagen I gene expressions. Mechanical properties of biofunctionalized CPC matched the reported strength and elastic modulus of cancellous bone.

Significance—A new class of biofunctionalized CPCs was developed, including CPC-RGD, CPC-Fn, CPC-FEPP, CPC-Geltrex, and CPC-Platelets. hUCMSCs on biofunctionalized CPCs had cell density, cell proliferation, actin fiber density, and bone mineralization that were dramatically better than those on traditional CPC. Novel biofunctionalized CPC scaffolds with greatly

Corresponding author: Hockin Xu, Professor, Director of Biomaterials & Tissue Engineering Division, University of Maryland Dental School, 650 West Baltimore Street, Baltimore, MD 21201, USA. Phone: 410 706 7047. Fax: 410 706 3028. hxu@umaryland.edu.

enhanced human stem cell proliferation and differentiation are promising to facilitate bone regeneration in a wide range of dental, craniofacial and orthopedic applications.

Keywords

Human umbilical cord stem cells; biofunctionalized calcium phosphate cement; RGD; fibronectin; osteogenic differentiation; dental and craniofacial repairs

1. Introduction

More than six million bone fractures occur every year in the USA, and the need for bone repair is increasing as the population ages [1-3]. Tissue engineering approaches are being developed to meet this tremendous need [4-6]. Stem cells and scaffolds are promising for tissue regeneration applications [7-10]. While mesenchymal stem cells (MSCs) are useful [4,5,10], the potency of bone marrow-derived MSCs decreases due to aging and diseases. Human umbilical cord MSCs (hUCMSCs) are a young and potent cell source, can be harvested without an invasive procedure, and are inexpensive and inexhaustible [11,12]. hUCMSCs can differentiate into adipocytes, osteoblasts, chondrocytes, neurons, etc. [11-16]. Recently, hUCMSCs were seeded with calcium phosphate (CaP) scaffolds for bone tissue engineering applications [16,17].

Hydroxyapatite (HA) and other CaP bioceramics are important for dental, craniofacial and orthopedic repairs due to their similarity to bone minerals and can bond to bone to form a functional interface [18-21]. Calcium phosphate cements can be injected and set *in situ* to achieve intimate adaptation to complex-shaped defects [18,19,22-27]. The first calcium phosphate cement (referred to as CPC) consisted of tetracalcium phosphate and dicalcium phosphate anhydrous, and was shown to be promising for dental and craniofacial repairs [22,28]. In addition, other calcium phosphate cements were developed with different compositions [18,19,23-27]. Stem cell-seeded CPC scaffolds were also being investigated [17].

Previous studies showed that human stem cell attachment to CPC was relatively poor [29,30]. Biofunctional agents such as fibronectin (Fn) and Arg-Gly-Asp (RGD) could improve cell attachment [31-35]. Therefore, in the present study, five types of biofunctional agents were incorporated into CPC. The first type is RGD, a known integrin-recognition site to promote cell attachment [33-35]. The second type is Fn, which is a general cell adhesion molecule that can anchor cells to collagen and proteoglycan [31,32]. Genetically-engineered proteins, such as fibronectin-like engineered protein polymer (FEPP), can also enhance cell adhesion [36,37]. FEPP includes 13 copies of the cell attachment epitope of Fn between repeated structural peptides. It has a stable three-dimensional (3D) conformation resistant to thermal and chemical denaturation. FEPP was selected as the third type. In addition, extracellular matrices (ECMs) can enhance stem cell function [38,39]. Geltrex is a 3D basement membrane ECM, which is a soluble form of reduced growth factor basement extract and consists of laminin, collagen IV, entactin, and heparin sulfate proteoglycan. Geltrex was selected as the forth type of biofunctional agent. The fifth type is platelet concentrate, which is a fraction of the plasma in which platelets are concentrated [40,41]. It is obtained by withdrawing blood from the vein of the patient. Platelet concentrate contains many bioactive molecules and was used in pre-formed bioceramics to improve cell proliferation [40,41]. Several previous studies incorporated transforming growth factor (TGF), bone morphogenetic protein (BMP), essential amino acids, and glucosamine into CPC [42-45]. However, a literature search revealed no report on using the aforementioned five types of biofunctional agents in CPC.

The objectives of this study were to develop novel biofunctionalized CPCs via incorporation of RGD, Fn, FEPP, Geltrex, and platelet concentrate and to investigate their effects on hUCMSC attachment and osteogenic differentiation for the first time. It was hypothesized that: (1) The incorporation of biofunctional agents in CPC will greatly enhance hUCMSCs attachment, proliferation and osteogenic differentiation; (2) The incorporation of biofunctional agents will not compromise the setting time and mechanical properties of CPC.

2. Materials and Methods

2.1. Fabrication of biofunctionalized CPC

Tetracalcium phosphate [TTCP: $Ca_4(PO_4)_2O$] was synthesized using dicalcium phosphate anhydrous (DCPA: CaHPO4) and calcium carbonate (J.T. Baker, Philipsburg, NJ). TTCP was ground to obtain particles of 1 to 80 μm, with a median of 17 μm [46,47]. DCPA was ground to obtain a median particle size of 1 μm. TTCP and DCPA powders were mixed at 1:1 molar ratio to form the CPC powder. Chitosan lactate (Vanson, Redmond, WA) was mixed with water at a chitosan/(chitosan + water) mass fraction of 15% to form the liquid, which could cause CPC to set fast [46]. For mechanical reinforcement, a resorbable suture fiber (Vicryl, polyglactin 910, Ethicon, NJ) was cut to filaments of a length of 3 mm and mixed with CPC paste at a fiber volume fraction 20%, following a previous study [17]. The CPC powder to liquid mass ratio of 2:1 was used to form a flowable paste. This CPC is referred to as “CPC control”.

Five biofunctionalized CPCs were prepared by incorporating the following biofunctional agents: RGD, Fn, FEPP, Geltrex, and platelet concentrate. Each biofunctional agent was mixed with the chitosan liquid, which was then mixed with the CPC powder. The concentration of RGD (Sigma, St. Louis, MO) was 50 μg RGD per 1 g of CPC paste (0.005% by mass), following a previous study [34]. For Fn (human plasma Fn, Invitrogen, Carlsbad, CA) and FEPP (Sigma), the same 0.005% concentration was used in CPC. Geltrex (Invitrogen) was added to CPC at 100 μL Geltrex per 1 g of CPC paste (0.1% by mass). This percentage was selected because preliminary study showed that it did not compromise the CPC setting time and mechanical property, while greatly improving cell function. Similarly, human platelet concentrate (1.2×10^6 platelets per μL, Biological Specialty, Colmar, PA) was added to CPC at 100 μL of platelet concentrate per 1 g of CPC paste (0.1% by mass). CPC containing these agents are referred to as CPC-RGD, CPC-Fn, CPC-FEPP, CPC-Geltrex, and CPC-Platelets, respectively.

2.2. Setting time and Mechanical Properties of biofunctionalized CPC

Setting time of CPC was measured using a previous method [46]. Briefly, CPC paste was filled into a mold of 3 × 4 × 25 mm and placed in a humidor at 37 °C. At one minute intervals, the specimen was scrubbed gently with figures until the powder component did not come off, indicating that the setting reaction had occurred sufficiently to hold the specimen together. The time measured from the powder-liquid mixing to this point was used as the setting time [46].

To measure mechanical properties, the paste was placed into a mold of 3 × 4 × 25 mm. The specimens were incubated at 37 °C for 4 h in a humidor, and then demolded and immersed in water at 37 °C for 20 h. The specimens were then fractured in three-point flexure with a span of 20 mm at a crosshead speed of 1 mm/min on a Universal Testing Machine (5500R, MTS, Cary, NC). Flexural strength and elastic modulus were measured (n = 6) [17,47]. Specimens were tested within a few minutes after being taking out of the water, and fractured while still being wet.

2.3. hUCMSC Culture and Proliferation

hUCMSCs (ScienCell, Carlsbad, CA) were derived from the Wharton's Jelly in umbilical cords of healthy babies and harvested as previously described [11,14]. The use of hUCMSCs was approved by the University of Maryland. Cells were cultured in a low-glucose Dulbecco's modified Eagle's medium (DMEM) supplemented with 10% fetal bovine serum (FBS) and 1% penicillin-streptomycin (Invitrogen), which is referred to as the control media. Passage 4 cells were used. The osteogenic media had 100 nM dexamethasone, 10 mM β-glycerophosphate, 0.05 mM ascorbic acid, and 10 nM 1α,25-Dihydroxyvitamin (Sigma) [17].

The materials for the preparation of CPC were sterilized in an ethylene oxide sterilizer (Andersen, Haw River, NC). Each CPC paste was filled into a disk mold with a diameter of 12 mm and a thickness of 1.5 mm. Each disk was incubated in the mold at 37 °C for 4 h in a humidor, and then demolded and immersed in water at 37 °C for 20 h. Each disk was placed in a well of a 24-well plate, and 50,000 cells in osteogenic medium was added to each well. After 1, 4, and 8 d, the constructs were washed in Tyrode's Hepes buffer, live/dead stained and viewed by epifluorescence microscopy (TE2000S, Nikon, Melville, NY) [17]. Images were taken at a magnification of 4 x. Three randomly-chosen fields of view were photographed for each disk. Five disks yielded 15 photos for each material at each time point. Live cells (stained green) and dead cells (stained red) were counted. The live cell density, D, is the number of live cells (N_L) attaching to the specimen divided by the surface area A: $D = N_L/A$ [17].

2.4. Fluorescence of actin fibers in hUCMSCs on biofunctionalized CPC

Actin fibers in the cell cytoskeleton were examined to determine if the biofunctional agents in CPC would enhance cell attachment and increase the amount of actin stress fibers. hUCMSCs were seeded at a relatively low density of 50,000 cells per well, the same as that for live/dead assay, in order to clearly see the stained cells and their actin fibers. The hUCMSC constructs after 1-day culture were washed with PBS, fixed with 4% parformaldehyde for 20 min, permeabilized with 0.1% Triton X-100 for 5 min, and blocked with 0.1% bovine serum albumin (BSA) for 30 min [48]. An actin cytoskeleton and focal adhesion staining kit (Chemicon, Temecula, CA) was used, which stained actin fibers into a red color. After incubating the construct with diluted (1:400) TRITC-conjugated phalloidin, cell nuclei were labeled with 4'-6-diamidino-2-phenylindole (DAPI), which revealed the nuclei in blue color. Fluorescence microscopy (Nikon) was used to examine the specimens. The fluorescence of actin fibers in hUCMSCs was measured via a NIS-Elements BR software (Nikon) [48].

2.5. Osteogenic Differentiation of hUCMSCs on biofunctionalized CPC

Quantitative real-time reverse transcription polymerase chain reaction (qRT-PCR, 7900HT, Applied Biosystems, Foster City, CA) was used. Each disk was placed in a well of a 24-well plate. A seeding density of 150,000 cells per well was used following previous studies [16,17,50]. The constructs were cultured in osteogenic media for 1, 4, and 8 d [15,17,50]. The total cellular RNA on the scaffolds was extracted with TRIzol reagent (Invitrogen). RNA (50 ng/μl) was reverse-transcribed into cDNA. TaqMan gene expression kits were used to measure the transcript levels of the proposed genes on human alkaline phosphatase (ALP, Hs00758162_m1), osteocalcin (OC, Hs00609452_g1), collagen type I (Coll I, Hs00164004), Runx2 (Hs00231692_m1) and glyceraldehyde 3-phosphate dehydrogenase (GAPDH, Hs99999905). Relative expression for each target gene was evaluated using the $2^{-\Delta\Delta Ct}$ method [49,50]. The C_t values of target genes were normalized by the C_t of the TaqMan human housekeeping gene GAPDH to obtain the ΔC_t values. These values were

subtracted by the Ct value of the hUCMSCs cultured on tissue culture polystyrene in the control media for 1 d (the calibrator) to obtain the $\Delta\Delta C_t$ values [17,49,50].

2.6. hUCMSC Mineralization on biofunctionalized CPC

Alizarin Red S (ARS) staining was used to examine mineralization by hUCMSCs [48,51]. hUCMSCs were seeded on CPC disks and cultured in osteogenic media. A seeding density of 150,000 cells per well was used following previous studies [16,17,50]. After 4, 14 and 21 d, the constructs were stained with ARS. An osteogenesis assay (Millipore, Billerica, MA) was used to measure the ARS concentration at OD_{405}, following the manufacturer's instructions. ARS standard curve was done with known concentration of the dye. CPC disks with the same composition and treatment, but without hUCMSC seeding, were also measured as control, and the control's ARS concentration was subtracted from the ARS concentration of the CPC scaffold with hUCMSCs [48]. This method yielded the net mineral concentration synthesized by the cells [48]. The time points of 14 d and 21 d were selected because previous studies found a large increase in calcium content from 12 d to 21 d [51].

2.7. Statistical analyses

One-way and two-way ANOVA were performed to detect significant effects of the variables. Tukey's multiple comparison procedures were used to group and rank the measured values, and Dunn's multiple comparison tests were used on data with non-normal distribution or unequal variance, both at a family confidence coefficient of 0.95.

3. Results

Fig. 1 plots the physical properties of biofunctionalized CPC: (A) cement setting time, (B) flexural strength, and (C) elastic modulus (mean ± SD; n = 6). The setting time was not significantly increased with the addition of RGD, Fn, and FEPP, while that with Geltrex and Platelets was slightly increased ($p < 0.05$). The flexural strength was not significantly changed with the addition of biofunctional agents ($p > 0.1$). Elastic moduli were also similar for all the groups ($p > 0.1$).

Fig. 2 shows live/dead images and cell density. Representative examples are shown in (A-C) at 1 d for CPC control, CPC-RGD, and CPC-FEPP, respectively, while 8 d images are shown in (D-F). CPC-Fn, CPC-Geltrex and CPC-Platelets had similar images to CPC-RGD, and therefore are not included here. Live cells were stained green and were numerous. Dead cells were stained red and were few (not included). Adding biofunctional agents into CPC increased the number of live cells, compared to CPC control. Cell proliferation from 1 to 8 d was faster on biofunctional CPC than CPC control. The quantification of live cell density is plotted in (G) (mean ± sd; n = 5). Cell density was increased by nearly 9-fold from 1 to 8 d on CPC-RGD, CPC-Fn and CPC-Platelets. At 8 d, cell density on CPC-RGD, CPC-Fn, CPC-Geltrex and CPC-Platelets ranged from 600 to 700 cells/mm^2, which was an order of magnitude higher than the 65 cells/mm^2 on CPC control ($p < 0.05$).

Fig. 3 shows the fluorescence of actin fibers. The actin fibers in the cell cytoskeleton were stained a red color. The cell nuclei appeared blue. Compared to CPC control in (A), the red fluorescence was greater in CPC with biofunctional agents (B-F), indicating an increased number of actin stress fibers. Extensive networks of actin stress fibers were observed in CPC with biofunctional agents. In (G), the area of red fluorescence was measured for each image and divided by the image area to yield the area fraction. Compared to CPC control, the actin fiber fluorescence area fraction was increased by 5-7 fold due to the biofunctional agents in CPC. In (H), the fluorescence intensity of actin fibers was normalized by the cell numbers for each material. Each value is mean ± sd (n = 5), and values indicated by different letters are significantly different ($p < 0.05$).

Osteogenic gene expressions are plotted in Fig. 4 for: (A) ALP, (B) Runx2, (C) OC, and (D) collagen I. In (A), ALP greatly increased at 8 d. Compared to CPC control, the ALP peak was much higher for all five biofunctionalized CPCs. CPC-Platelets had the highest ALP ($p < 0.05$). In (B), Runx2 had a similar trend as ALP, with all five biofunctionalized CPCs having higher values at 8 d than CPC control. CPC-Platelets had the highest Runx2. In (C) and (D), both OC and collagen I were greatly increased at 8 d. The OC and collagen I peaks were much higher for biofunctionalized CPCs than CPC control ($p < 0.05$).

hUCMSC mineralization is shown in Fig. 5. ARS stained minerals into a red color. In (A), typical staining photos are shown for CPC control, CPC-Fn and CPC-Platelets at 4 d and 21 d, as examples. A thick matrix mineralization was synthesized by the cells at 21 d. ARS yielded a red color for CPC without cells, because CPC had minerals. However, for CPC with hUCMSCs, the red staining became much thicker over time. A layer of new mineral matrix synthesized by cells covered the disk, and the mineral staining increased with the addition of biofunctional agents in CPC. In (B), as measured by the osteogenesis assay, mineral synthesis by hUCMSCs at 21 d on CPC-Platelets was 3-fold the mineral synthesis by hUCMSCs on CPC control. CPC disks without hUCMSCs had baseline values of 0.5-0.7 mM. The values in (B) had their baseline values subtracted to represent the mineral synthesized by the hUCMSCs.

4. Discussion

CPC is promising for dental, craniofacial and orthopedic applications. However, human stem cell attachment to the traditional CPC is relatively poor. The present study developed novel biofunctionalized CPC scaffolds which greatly improved hUCMSC attachment, proliferation, osteogenic differentiation and mineralization. Extracellular matrix environments are essential for regulating cellular processes to promote tissue regeneration. In previous studies, Fn and RGD were coated on the surfaces of calcium phosphate bioceramics [33-35], which were prefabricated implants and different from the injectable CPC. There has been no report on developing biofunctionalized CPC by incorporating agents such as RGD and Fn into the CPC paste. The present study demonstrated that the new CPC-RGD, CPC-Fn, CPC-FEPP, CPC-Geltrex, and CPC-Platelet scaffolds all substantially enhanced the hUCMSC functions. Live cell density was greatly increased due to the incorporation of biofunctional agents into CPC. Actin stress fibers were also extensively increased. The actin stress fibers anchor to the cell membrane at focal adhesions which are connected to the extracellular matrix or the scaffold [48]. The mineralization by hUCMSCs was also markedly enhanced due to biofunctional agents in CPC. Therefore, mixing these biofunctional agents into CPC paste appears to be a feasible method to yield biofunctionalized CPC scaffolds to enhance cell function and bone regeneration.

RGD is the principle integrin-binding domain present in ECM proteins and is able to bind multiple integrin species, and hence is the most widely studied adhesive peptide in the development of biomimetic scaffolds [35]. Compared to native ECM proteins, RGD has less risk of immune reaction or pathogen transfer. Previous studies showed that RGD-coated HA implants enhanced MSC attachment and spreading, depending on RGD density [33]. In a rabbit model, RGD-grafted biphasic calcium phosphate ceramics induced more new bone than that without RGD [52]. Another cell adhesion molecule, Fn, is also an important ECM protein. It regulates many cellular functions and directs cell adhesion, proliferation, and differentiation via direct interactions with cell surface integrin receptors [31]. Fn is synthesized by the adherent cells which assemble into a fibrillar network through integrin-dependent and fibronectin-integrin interactions. In the present study, incorporating RGD or Fn into the CPC paste substantially enhanced hUCMSC attachment, actin stress fiber density, cell proliferation, and bone mineralization for the first time. This enhancement is

likely because some of the cell adhesion molecules were located on the CPC surface where the cells were seeded.

FEPP is genetically-engineered and has a three-dimensional structure [36,37]. Previous studies showed that FEPP-coated polyurethane graft significantly enhanced cell adhesion [37]. Geltrex is another three-dimensional membrane and a human-derived ECM that can support stem cell culture [38,39]. There has been no report of incorporating FEPP or Geltrex into a CPC paste. In the present study, the incorporation of FEPP and Geltrex into CPC improved cell attachment and spreading at 1 d, and cell proliferation at 8 d. Actin fiber organization in hUCMSCs on CPC-FEPP and CPC-Geltrex showed dense networks with cell-cell and cell-material attachment. This is consistent with the observation that on the CPC disks, the cells appeared to spread into different directions and formed three-dimensional networks on CPC-FEPP and CPC-Geltrex scaffolds. While the present study served as a preliminary screening study to examine the effects of the five different biofunctional agents, further study is needed to investigate the different mechanisms of cell function enhancement via each agent.

Platelet concentrate contains a mixture of growth factors which play an important role in wound healing and tissue regeneration [40,41]. Recently, an increasing trend has emerged in the use of autologous platelets to facilitate healing [53,54]. Platelets have many bioactive proteins responsible for attracting macrophages, MSCs and osteoblasts, which promote the removal of necrotic tissue and enhance tissue regeneration and healing. Platelet-rich plasma appears to be an effective additive in periodontal and oral surgical procedures including bone grafts, implants and maxillofacial reconstructions by facilitating the healing rate [53]. From the initial 30-60 mL of blood withdrawal from the vein, 3-6 mL of platelet-rich plasma can be collected, hence self-production of platelet-rich plasma can be achieved [53,54]. The promise of platelets is supported by the present study on platelet incorporation into CPC for the first time. hUCMSC attachment and spreading on CPC-Platelets were markedly improved over that of CPC control. This likely mediated subsequent cellular function and matrix formation. This is consistent with previous studies, which showed that the addition of platelet-rich plasma in calcium-deficient HA and beta-tricalcium phosphate showed an increased cell-loading capacity and proliferation [40]. Furthermore, the present study showed that CPC-Platelets had excellent cell proliferation and high actin fiber density, with bone mineralization being 3-fold that of CPC control.

Comparing the effects of the five different biofunctional agents, CPC-RGD, CPC-FN and CPC-Platelets had similarly good live cell density, which was better than CPC-FEPP and CPC-Geltrex. However, CPC-Platelets had the best osteogenic differentiation, manifested by the highest levels of ALP and Runx2 gene expressions among all six groups. These results are consistent with CPC-platelets having the most bone mineralization at 21 d. The mineral synthesis by the hUCMSCs in these six groups had this ranking: CPC-Platelets > CPC-RGD = CPC-Fn > CPC-FEPP = CPC-Geltrex > CPC control. The reason that CPC-Platelets resulted in the best hUCMSC osteogenic differentiation and mineral synthesis is likely that platelet concentrate contained a number of bioactive proteins and growth factors which enhanced cell differentiation. While biofunctional agents such as RGD and Fn mainly enhance cell adhesion, platelet concentrate with growth factors is expected to directly enhance cell differentiation. However, it should be noted that when cell attachment and cell density are increased via RGD and Fn, the cell functions and biosynthesis will also be enhanced due to cell-cell interactions and increased secretion by neighboring cells of extracellular matrix and proteins to enhance each other's function [17,50]. Further studies are needed to investigate the correlation between the specific growth factors in the platelet concentrate and the osteogenic differentiation of stem cells. This pilot study showed that simply mixing platelet concentrate with CPC to form a biofunctionalized paste resulted in

the best cell proliferation and osteogenic differentiation among the groups tested. Therefore, incorporating autologous platelets from the plasma of the patient into the CPC paste appears to be a promising approach to enhance cell attachment and bone regeneration. It should be noted that the present study examined five biofunctional agents in CPC, but used only one mass fraction for each agent. Each biofunctional agent mass fraction was selected based on previous studies and our preliminary experiments. Further study should systematically vary the biofunctional agent mass fraction in CPC and determine the corresponding hUCMSC response. Another issue is that the biofunctional agents were not chemically bonded to CPC. Therefore, the biofunctional agents in CPC could gradually diffuse away. The advantage of CPC is that, instead of biofunctional agent being coated on a preformed scaffold surface which could be lost easily, the biofunctional agent was mixed into the entire CPC paste. Hence, the biofunctional agent inside CPC could gradually diffuse to the surface to stimulate the attached cells. The results of the present study showed that the biofunctional agents significantly enhanced the osteogenic differentiation and mineral synthesis of hUCMSCs for up to 21 days. Further study is needed to measure and control the biofunctional agent release rate from CPC, and to investigate if the biofunctional agent duration in CPC is sufficient to enhance bone regeneration *in vivo*.

hUCMSCs are a relatively new stem cell source that is highly promising for tissue regeneration. It avoids the invasive procedure needed to harvest bone marrow MSCs. While attaching to CPCs, the ALP, Runx2, OC and collagen 1 gene expressions for hUCMSCs were all markedly increased at 8 d compared to 1 d. ALP and OC are frequently measured as key bone markers [13,14,21]. Runx2 is an important transcription gene with the osteogenic phenotype [50]. ECM-related cell structure collagen I gene is another maker for bone formation. Collagen I mediates cell adhesion and osteoblast phenotype formation, and provides a template for mineralization. During osteogenic differentiation, the genetic expressions of bone markers are upregulated. This sets off a cascade of events, which leads to the production of the extracellular matrix and bone minerals. Hence, mineralization occurs later than the gene expression peaks. Previous studies found a large increase in calcium content in the *in vitro* cell cultures between 12 to 21 d [51]. In the present study, the mineral staining color became a darker and thicker red at 21 d. Mineral synthesis by the cells on biofunctionalized CPCs was nearly 3-fold that of CPC control at 21 d. These results support the development of biofunctionalized CPCs and the use of hUCMSCs for bone tissue engineering applications. The present study seeded hUCMSCs on CPC disks without macropores as a pilot study. While the effects of biofunctional agents in CPC are expected to be the same, further study should create macropores in biofunctionalized CPC by using porogen to enhance cell infiltration and tissue ingrowth.

For potential applications such as periodontal bone repair and mandibular and maxillary ridge augmentation, the CPC implants would be subject to early loading by provisional dentures and need to be resistant to flexure. In addition, major reconstructions of the maxilla or mandible after trauma or tumor resection would benefit from a moldable implant such as CPC with good strength and rapid osteoconduction due to the seeding of stem cells. The support of metal dental implants or augmentation of deficient implant sites with CPC would also require fracture resistance. In addition, for growth factor delivery, *in vivo* loading may result in scaffold failure and the loss of growth factors by convective transport. For example, the protein was rapidly purged out of a collagen carrier under stresses *in vivo*, because the collagen sponge had no load-bearing capability [55]. Therefore, mechanical properties are needed for the CPC scaffold to provide a matrix for cell function, while maintaining the volume and supporting the external stresses. For comparison, previous studies have developed other types of injectable carriers for cell and growth factor delivery. For example, a previous study reported an injectable polymeric carrier for cell delivery, with a strength of 0.7 MPa [56]. Hydrogels for cell delivery had strengths of about 0.1 MPa [57,58]. While

these systems are useful for non-load-bearing applications, their strengths are much lower than the reported strength of about 3.5 MPa for cancellous bone [59]. Regarding elastic modulus, previous studies reported that injectable polymeric carriers for cell delivery had a modulus of about 8 MPa [56]. In comparison, the biofunctionalized CPCs had moduli of about 150 MPa, matching the reported modulus of 50-300 MPa for cancellous bone [60]. Therefore, the novel biofunctionalized CPCs with flexural strengths of about 10 MPa and elastic modulus of 150 MPa are promising for use in a wide range of dental, craniofacial and orthopedic applications. Further study is needed to investigate the *in vivo* bone regeneration via the novel biofunctionalized CPC scaffolds in animal models.

5. Conclusions

A new class of biofunctionalized CPCs was developed by incorporation of five biofunctional agents: RGD, Fn, FEPP, Geltrex, and platelets. Substantially enhanced human stem cell attachment, proliferation, and bone mineral synthesis were obtained. Literature search revealed no report on incorporating these five biofunctional agents into CPC. Marked improvements in hUCMSC proliferation, actin stress fiber density, and osteogenic differentiation were achieved on biofunctionalized CPCs, compared to CPC control. ALP, Runx2, OC, and collagen I gene expressions were highly elevated at 8 d. A thick layer of bone mineral matrix was synthesized by the hUCMSCs at 21 d. hUCMSC mineralization on biofunctionalized CPCs was nearly 3-fold that on CPC control. The mechanical properties of the biofunctionalized CPCs matched or exceeded those of cancellous bone. The stem cell-seeded biofunctionalized CPCs with greatly enhanced cell proliferation and osteogenic differentiation is promising to promote bone regeneration in a wide range of dental, craniofacial and orthopedic applications.

Acknowledgments

We thank Dr. Michael D. Weir for experimental help and discussions on making the scaffolds. We also thank Drs. L. C. Chow and S. Takagi at the Paffenbarger Research Center, and Dr. Carl G. Simon at the National Institute of Standards and Technology for discussions and help. This study was supported by NIH R01 grants DE14190 and DE17974 (HX), Maryland Stem Cell Fund (HX), and the University of Maryland Dental School.

References

1. WHO Technical Report Series 919. The burden of musculoskeletal conditions at the start of the new millennium. Geneva, Switzerland: WHO; 2003. p. 102-103.
2. Johnson PC, Mikos AG, Fisher JP, Jansen JA. Strategic directions in tissue engineering. Tissue Eng. 2007; 13:2827–2837. [PubMed: 18052823]
3. Mao, JJ.; Vunjak-Novakovic, G.; Mikos, AG.; Atala, A. Regenerative medicine: Translational approaches and tissue engineering. Boston, MA: Artech House; 2007.
4. Foppiano S, Marshall SJ, Marshall GW, Saiz E, Tomsia AP. The influence of novel bioactive glasses on in vitro osteoblast behavior. J Biomed Mater Res A. 2004; 71:242–249. [PubMed: 15372470]
5. Benoit DSW, Nuttelman CR, Collins SD, Anseth KS. Synthesis and characterization of a fluvastatin-releasing hydrogel delivery system to modulate hMSC differentiation and function for bone regeneration. Biomaterials. 2006; 27:6102–6110. [PubMed: 16860387]
6. Simon CG, Lin-Gibson S. Combinatorial and high-throughput screening of biomaterials. Advanced Mater. 2011; 23:369–387.
7. Jansen JA, Vehof JW, Ruhe PQ, Kroeze-Deutman H, Kuboki Y, Takita H, et al. Growth factor-loaded scaffolds for bone engineering. J Controlled Release. 2005; 101:127–136.
8. Mikos AG, Herring SW, Ochareon P, Elisseeff J, Lu HH, Kandel R, et al. Engineering complex tissues. Tissue Eng. 2006; 12:3307–3339. [PubMed: 17518671]

9. Mao JJ, Giannobile WV, Helms JA, Hollister SJ, Krebsbach PH, Longaker MT. Craniofacial tissue engineering by stem cells. J Dent Res. 2006; 85:966–979. [PubMed: 17062735]
10. Huebsch N, Arany PR, Mao AS, Shvartsman D, Ali AO, Bencherif SA, et al. Harnessing traction-mediated manipulation of the cell/matrix interface to control stem-cell fate. Nat Mater. 2010; 9:518–526. [PubMed: 20418863]
11. Wang HS, Hung SC, Peng ST. Mesenchymal stem cells in the Wharton's jelly of the human umbilical cord. Stem Cells. 2004; 22:1330–1337. [PubMed: 15579650]
12. Baksh D, Yao R, Tuan RS. Comparison of proliferative and multilineage differentiation potential of human mesenchymal stem cells derived from umbilical cord and bone marrow. Stem Cells. 2007; 25:1384–1392. [PubMed: 17332507]
13. Wang L, Singh M, Bonewald LF, Detamore MS. Signaling strategies for osteogenic differentiation of human umbilical cord mesenchymal stromal cells for 3D bone tissue engineering. J Tissue Eng Regen Med. 2009; 3:398–404. [PubMed: 19434662]
14. Weiss ML, Medicetty S, Bledsoe AR, Rachakatla RS, Choi M, Merchav S, et al. Human umbilical cord matrix stem cells: Preliminary characterization and effect of transplantation in a rodent model of Parkinson's disease. Stem Cells. 2006; 24:781–792. [PubMed: 16223852]
15. Bailey MM, Wang L, Bode CJ, Mitchell KE, Detamore MS. A comparison of human umbilical cord matrix stem cells and temporomandibular joint condylar chondrocytes for tissue engineering temporomandibular joint condylar cartilage. Tissue Eng. 2007; 13:2003–2010. [PubMed: 17518722]
16. Zhao L, Weir MD, Xu HHK. Human umbilical cord stem cell encapsulation in calcium phosphate scaffolds for bone engineering. Biomaterials. 2010; 31:3848–3857. [PubMed: 20149437]
17. Zhou H, Weir MD, Xu HHK. Effect of cell seeding density on proliferation and osteodifferentiation of umbilical cord stem cells on calcium phosphate cement-fiber scaffold. Tissue Eng Part A. 2011; 17:2603–2613. [PubMed: 21745111]
18. Ginebra MP, Driessens FC, Planell JA. Effect of the particle size on the micro and nanostructural features of a calcium phosphate cement: a kinetic analysis. Biomaterials. 2004; 25:3453–62. [PubMed: 15020119]
19. Bohner M, Baroud G. Injectability of calcium phosphate pastes. Biomaterials. 2005; 26:1553–1563. [PubMed: 15522757]
20. Deville S, Saiz E, Nalla RK, Tomsia AP. Freezing as a path to build complex composites. Science. 2006; 311:515–518. [PubMed: 16439659]
21. Reilly GC, Radin S, Chen AT, Ducheyne P. Differential alkaline phosphatase responses of rat and human bone marrow derived mesenchymal stem cells to 45S5 bioactive glass. Biomaterials. 2007; 28:4091–4097. [PubMed: 17586040]
22. Brown, WE.; Chow, LC. A new calcium phosphate water setting cement. In: Brown, PW., editor. Cements research progress. Westerville, OH: Am Ceram Soc; 1986. p. 352-379.
23. Ginebra MP, Rilliard A, Fernández E, Elvira C, Román JS, Planell JA. Mechanical and rheological improvement of a calcium phosphate cement by the addition of a polymeric drug. J Biomed Mater Res. 2001; 57:113–118. [PubMed: 11416857]
24. Barralet JE, Gaunt T, Wright AJ, Gibson IR, Knowles JC. Effect of porosity reduction by compaction on compressive strength and microstructure of calcium phosphate cement. J Biomed Mater Res. 2002; 63B:1–9. [PubMed: 11787022]
25. Bohner M, Gbureck U, Barralet JE. Technological issues for the development of more efficient calcium phosphate bone cements: a critical assessment. Biomaterials. 2005; 26:6423–9. [PubMed: 15964620]
26. Kasten P, Beyen I, Niemeyer P, Luginbuhl R, Bohner M, Richter W. Porosity and pore size of beta-tricalcium phosphate scaffold can influence protein production and osteogenic differentiation of human mesenchymal stem cells: an *in vitro* and *in vivo* study. Acta Biomater. 2008; 4:1904–1915. [PubMed: 18571999]
27. Bohner M. Design of ceramic-based cements and putties for bone graft substitution. Eur Cell Mater. 2010; 20:1–12. [PubMed: 20574942]

28. Friedman CD, Costantino PD, Takagi S, Chow LC. BoneSource hydroxyapatite cement: a novel biomaterial for craniofacial skeletal tissue engineering and reconstruction. J Biomed Mater Res. 1998; 43:428–432. [PubMed: 9855201]
29. Link DP, van den DJ, Wolke JG, Jansen JA. The cytocompatibility and early osteogenic characteristics of an injectable calcium phosphate cement. Tissue Eng. 2007; 13:493–500. [PubMed: 17362133]
30. Weir MD, Xu HHK. Culture human mesenchymal stem cells with calcium phosphate cement scaffolds for bone repair. J Biomed Mater Res B. 2010; 93:93–105.
31. Mosher, DF. Fibronectin. San Diego, CA: Academic Press; 1989.
32. van den Dolder J, Bancroft GN, Sikavitsas VI, Spauwen PH, Mikos AG, Jansen JA. Effect of fibronectin- and collagen I-coated titanium fiber mesh on proliferation and differentiation of osteogenic cells. Tissue Eng. 2003; 9:505–515. [PubMed: 12857418]
33. Sawyer AA, Hennessy KM, Bellis SL. Regulation of mesenchymal stem cell attachment and spreading on hydroxyapatite by RGD peptides and adsorbed serum proteins. Biomaterials. 2005; 26:1467–1475. [PubMed: 15522748]
34. Schneiders W, Reinstorf A, Pompe W, Grass R, Biewener A, Holch M, et al. Effect of modification of hydroxyapatite/collagen composites with sodium citrate, phosphoserine/RGD-peptide and calcium carbonate on bone remodeling. Bone. 2007; 40:1048–1059. [PubMed: 17223400]
35. Bellis SL. Advantages of RGD peptides for directing cell association with biomaterials. Biomaterials. 2011; 32:4205–4210. [PubMed: 21515168]
36. Esty A. Receptor-specific serum-free cell attachment using a high stable engineered protein polymer. Am Biotechnol Lab. 1991; 9:44. [PubMed: 1367292]
37. Tiwari A, Kidane A, Salacinski H, Punshon G, Hamilton G, Seifalian AM. Improving endothelial cell retention for single stage seeding of prosthetic grafts: use of polymer sequences of arginine-glycine-aspartate. Eur J Vasc Endovasc Surg. 2003; 25:325–329. [PubMed: 12651170]
38. Ilic D. Culture of human embryonic stem cells and the extracellular matrix microenviroment. Regen Med. 2006; 1:95–101. [PubMed: 17465823]
39. Kim J, Efe JA, Zhu S, Talantova M, Yuan X, Wang S, et al. Direct reprogramming of mouse fibroblasts to neural progenitors. Proc Nat Acad Sci USA. 2011 10.1073,1103113108 [Epub ahead of print].
40. Vogel JP, Szalay K, Geiger F, Kramer M, Richter W, Kasten P. Platelet-rich plasma improves expansion of human mesenchymal stem cells and retains differentiation capacity and in vivo bone formation in calcium phosphate ceramics. Platelets. 2006; 17:462–469. [PubMed: 17074722]
41. Kasten P, Vogel J, Beyen I, Weiss S, Niemeyer P, Leo A, et al. Effect of platelet-rich plasma on the in vitro proliferation and osteogenic differentiation of human mesenchymal stem cells on distinct calcium phosphate scaffolds: the specific surface area makes a difference. J Biomater Appl. 2008; 23:169–188. [PubMed: 18632770]
42. Blom EJ, Klein-Nulend J, Wolke JGC, van Waas MAJ, Driessens FCM, Burger EH. Transforming growth factor-b1 incorporation in a calcium phosphate bone cement: Material properties and release characteristics. J Biomed Mater Res. 2002; 59:265–272. [PubMed: 11745562]
43. Vater C, Lode A, Bernhardt A, Reinstorf A, Nies B, Gelinsky M. Modifications of a calcium phosphate cement with biomolecules - influence on nanostructure, material, and biological properties. J Biomed Mater Res. 2010; 95:912–923.
44. Ginebra MP, Traykova T, Planell JA. Calcium phosphate cements as bone drug delivery systems: A review. J Control Release. 2006; 113:102–110. [PubMed: 16740332]
45. Sawamura, T.; Hattori, M.; Okuyama, M. Calcium phosphate cements and calcium phosphate cement compositions. U S Patent No. 6,051,061. 2000.
46. Xu HHK, Takagi S, Quinn JB, Chow LC. Fast-setting calcium phosphate scaffolds with tailored macropore formation rates for bone regeneration. J Biomed Mater Res. 2004; 68:725–734.
47. Xu HHK, Simon CG. Self-hardening calcium phosphate composite scaffold for bone tissue engineering. J Orthop Res. 2004; 22:535–543. [PubMed: 15099632]
48. Thein-Han WW, Xu HHK. Collagen-calcium phosphate cement scaffolds seeded with umbilical cord stem cells for bone tissue engineering. Tissue Eng A. 2011; 17:2943–2954.

49. Livak KJ, Schmittgen TD. Analysis of relative gene expression data using real-time quantitative PCR and the $2^{-\Delta\Delta Ct}$ Method. Methods. 2001; 25:402–408. [PubMed: 11846609]
50. Kim K, Dean D, Mikos AG, Fisher JP. Effect of initial cell seeding density on early osteogenic signal expression of rat bone marrow stromal cells cultured on cross-linked poly(propylene fumarate) disks. Biomacromolecules. 2009; 10:1810–1817. [PubMed: 19469498]
51. Wang YH, Liu Y, Maye P, Rowe DW. Examination of mineralized nodule formation in living osteoblastic cultures using fluorescent dyes. Biotechnol Prog. 2006; 22:1697–1701. [PubMed: 17137320]
52. Fricain JC, Pothuaud L, Durrieu MC, Pallu S, Bareille R, Renard M, et al. Effects of cyclic RGD peptide functionalization on the quantitative bone ingrowth process in cellularized biphasic calcium phosphate ceramics. Key Eng Mater. 2005; 284-286:647–650.
53. Carlson NE, Roach RB. Platelet-rich plasma: clinical applications in dentistry. J Am Dent Assoc. 2002; 133:1383–1386. [PubMed: 12403541]
54. Sampson S, Gerhardt M, Mandelbaum B. Platelet rich plasma injection grafts for musculoskeletal injuries: a review. Curr Rev Musculoskelet Med. 2008; 1:165–174. [PubMed: 19468902]
55. Martin GJ, Boden SD, Marone MA, Moskovitz PA. Posterolateral intertransverse process spinal arthrodesis with rhBMP-2 in a nonhuman primate: important lessons learned regarding dose, carrier, and safety. J Spinal Disord. 1999; 12:179–186. [PubMed: 10382769]
56. Shi X, Sitharaman B, Pham QP, Liang F, Wu K, Billups WE, et al. Fabrication of porous ultra-short single-walled carbon nanotube nanocomposite scaffolds for bone tissue engineering. Biomaterials. 2007; 28:4078–4090. [PubMed: 17576009]
57. Kuo CK, Ma PX. Ionically crosslinked alginate hydrogels as scaffolds for tissue engineering: Part I. Structure, gelation rate and mechanical properties. Biomaterials. 2001; 22:511–521. [PubMed: 11219714]
58. Drury JL, Dennis RG, Mooney DJ. The tensile properties of alginate hydrogels. Biomaterials. 2004; 25:3187–3199. [PubMed: 14980414]
59. Damien CJ, Parsons JR. Bone graft and bone graft substitutes: A review of current technology and applications. J Appl Biomater. 1991; 2:187–208. [PubMed: 10149083]
60. O'Kelly K, Tancred D, McCormack B, Carr A. A quantitative technique for comparing synthetic porous hydroxyapatite structure and cancellous bone. J Mater Sci: Mater in Med. 1996; 7:207–213.

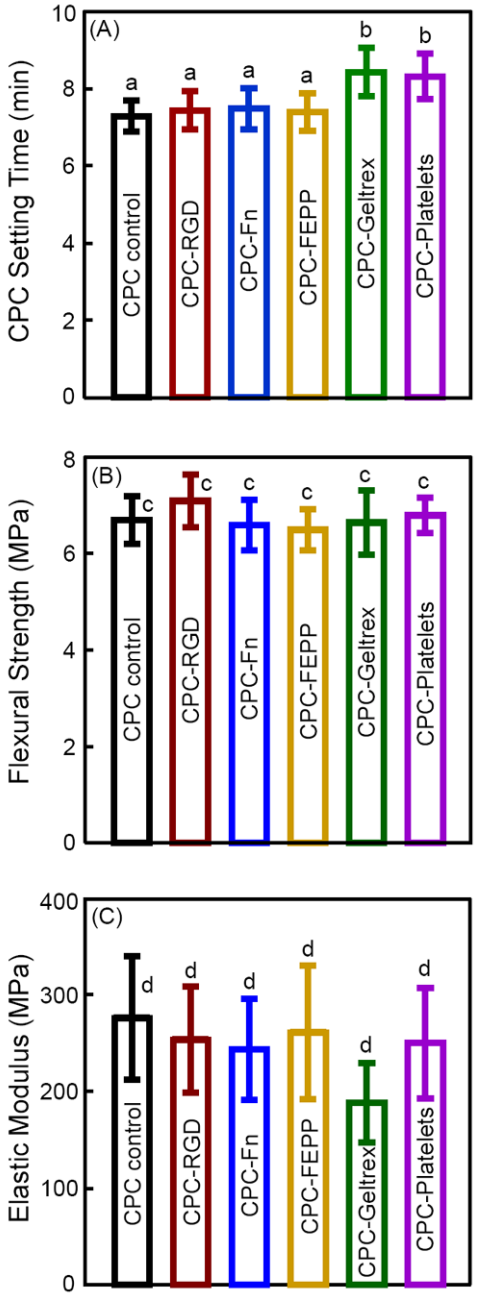

Figure 1.

Physical properties of biofunctionalized CPCs. (A) Cement setting time (mean ± sd; n = 3), (B) flexural strength (mean ± sd; n = 6), and (C) elastic modulus (mean ± sd; n = 6). In each plot, bars of values with the same letters are not significantly different ($p > 0.1$).

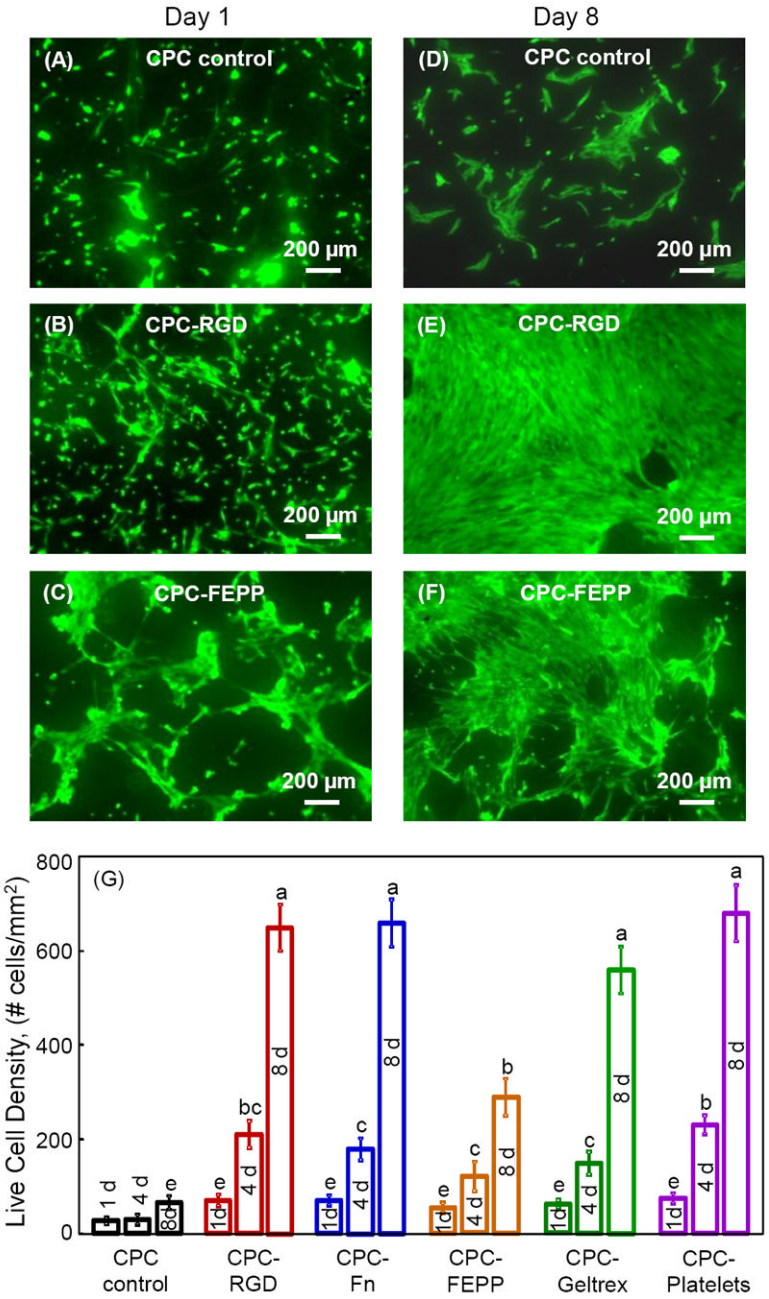

Figure 2.

Live/dead staining of hUCMSCs on CPC. Live cells showed green fluorescence. Dead cells were stained red. There were numerous live cells and very few dead cells (not shown). (A-C) CPC control, CPC-RGD, and CPC-FEPP, respectively, at 1 d. (D-F) CPC control, CPC-RGD, and CPC-FEPP, respectively, at 8 d. CPC-Fn, CPC-Geltrex and CPC-Platelets had similar images to CPC-RGD, and therefore are not included here. Incorporation of biofunctional agents into CPC increased the number of live cells, compared to CPC control. (G) Live cell density (mean ± sd; n = 5). hUCMSCs proliferated well on all CPC scaffolds, with cell density greatly increasing from 1 to 8 d. At 8 d, cell density on CPC-RGD, CPC-Fn, CPC-Geltrex and CPC-Platelets was 600-700 cells/mm^2, nearly 10-fold of the 65 cells/mm^2 on CPC control. Values with dissimilar letters are significantly different ($p < 0.05$).

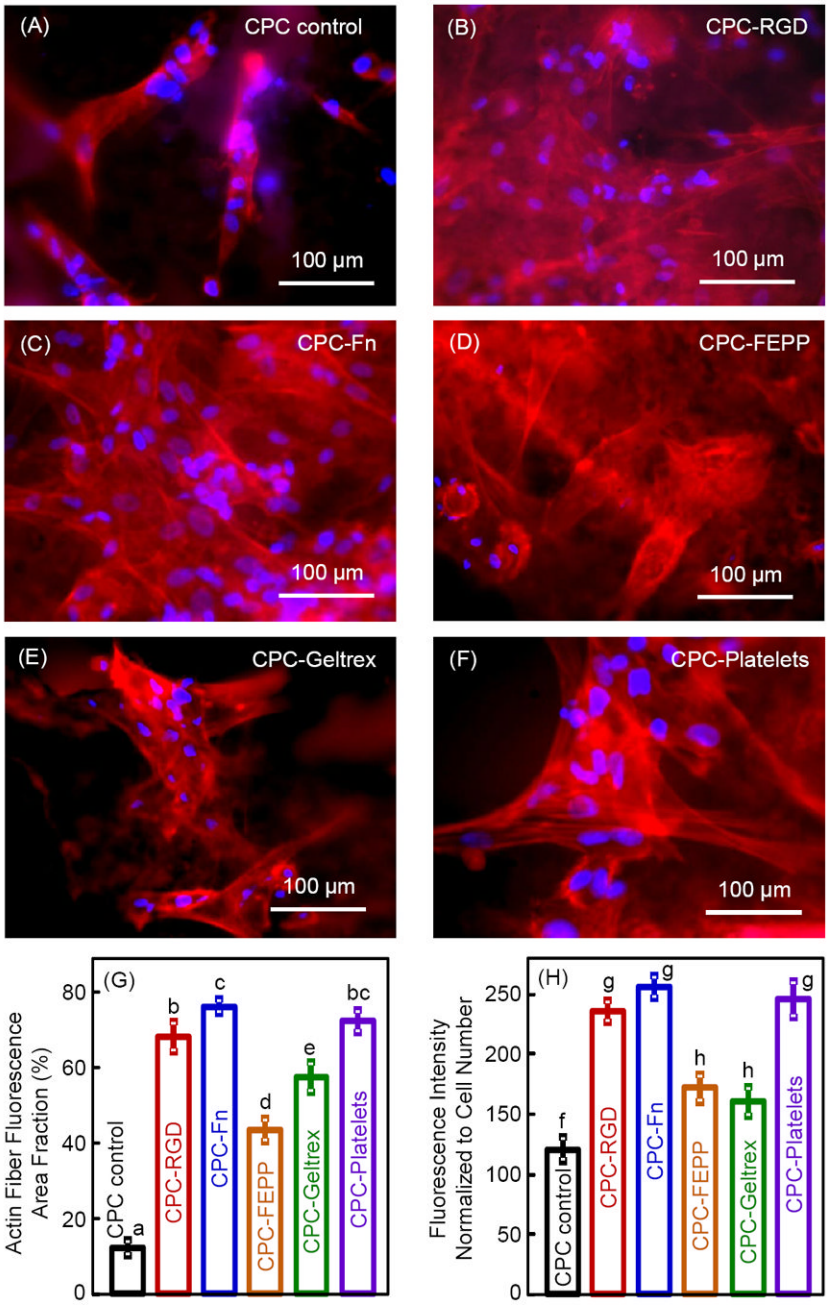

Figure 3.

Fluorescence of actin fibers in hUCMSCs at 1 d on (A-F) CPC control, CPC-RGD, CPC-Fn, CPC-FEPP, CPC-Geltrex, and CPC-Platelets, respectively. Actin stress fibers in hUCMSCs were stained red. Cell nuclei (blue fluorescence) indicated the location and distribution of the hUCMSCs on the scaffold. The red color was brighter and denser with the addition of biofunctional agents in CPC. (G) Actin fiber fluorescence area fraction. The area of fluorescence for actin fibers was divided by the total area of the photo. (H) Fluorescence intensity of actin fibers was normalized by cell numbers. Each value is mean ± sd; n = 5. Values with dissimilar letters are significantly different ($p < 0.05$).

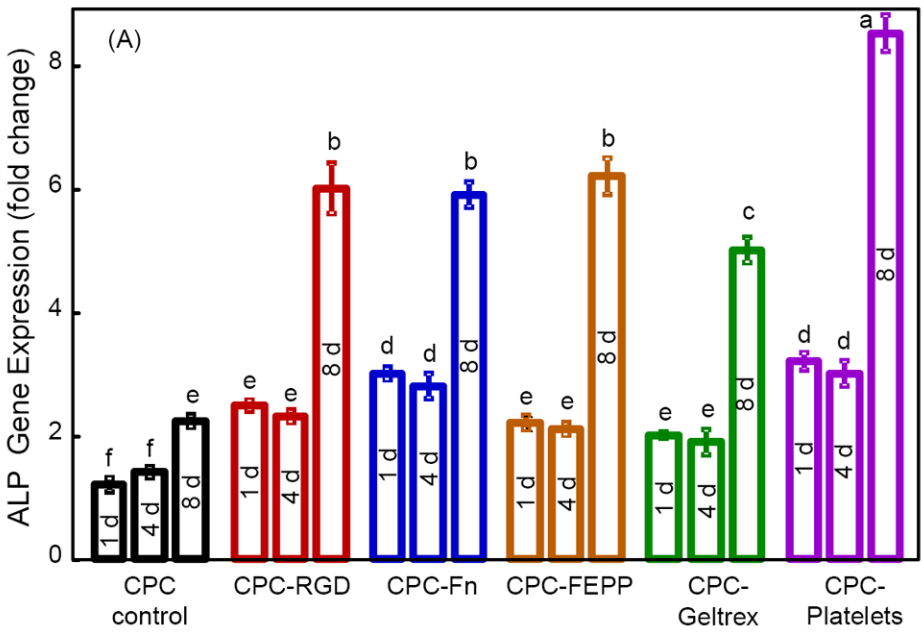

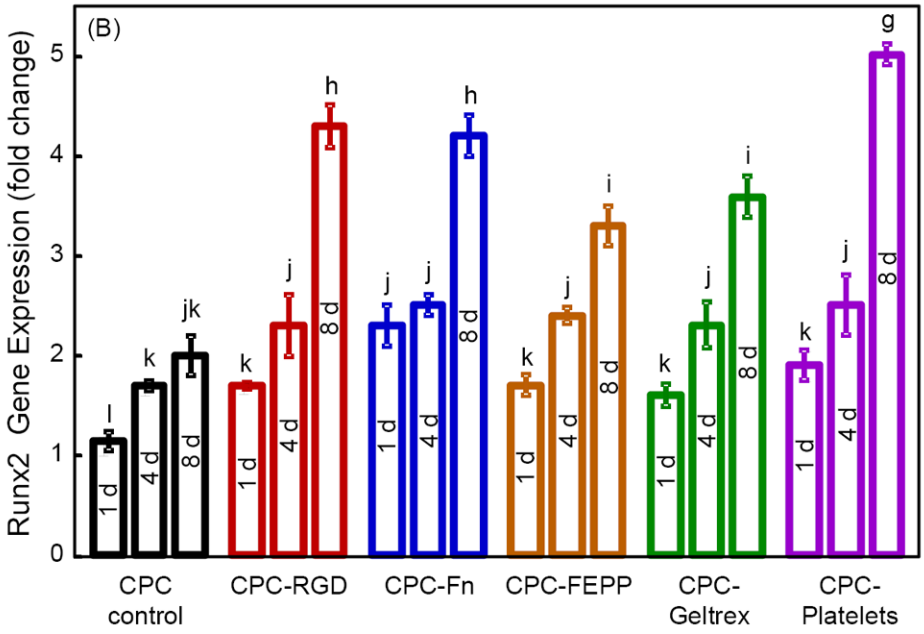

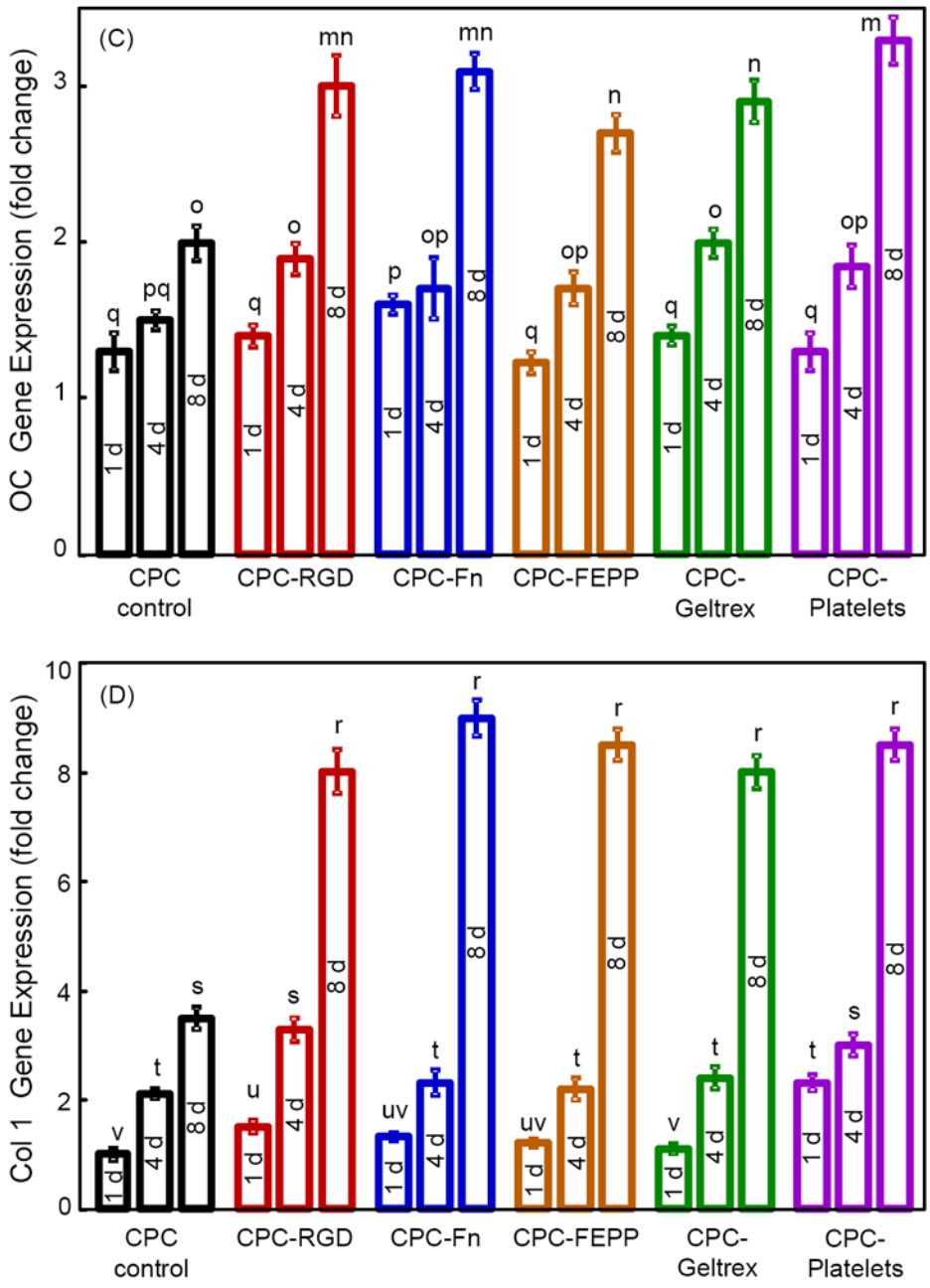

Figure 4.

RT-PCR of osteogenic differentiation of hUCMSCs on biofunctionalized CPCs. (A) ALP, (B) Runx2, (C) OC, (D) collagen I gene expressions. Each value is mean ± sd; n = 5. In each plot, values with dissimilar letters are significantly different ($p < 0.05$).

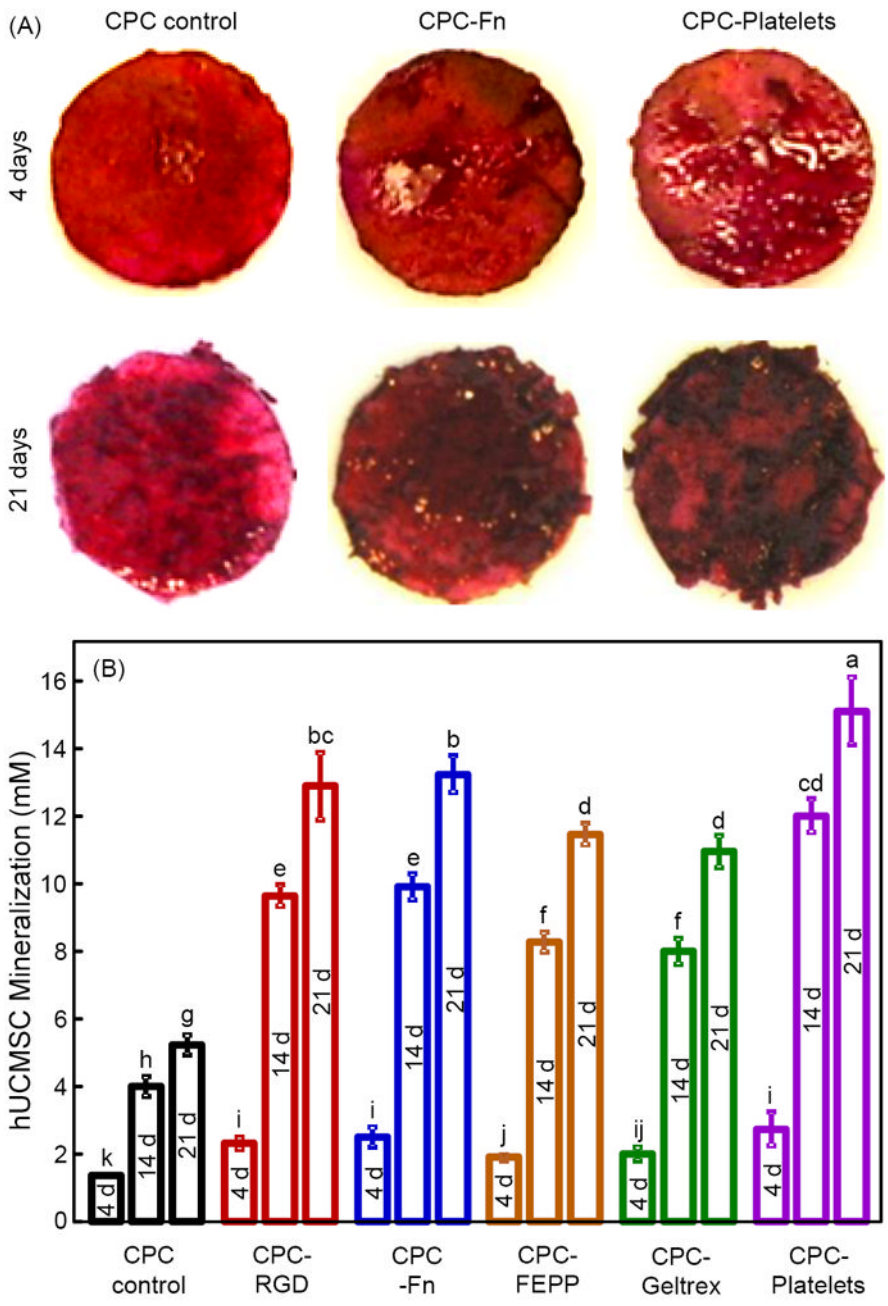

Figure 5.

Mineral synthesis by hUCMSCs on biofunctionalized CPCs. ARS stained minerals into a red color. (A) ARS staining of hUCMSC-scaffold constructs after 4 d and 21 d, on CPC control, CPC-Fn, and CPC-Platelets, as examples. For all materials, the mineral staining became a thicker and darker red with increasing time from 4 d to 21 d. Between materials, mineralization was thicker and denser on biofunctionalized CPCs than that on CPC control. (B) Mineral concentration synthesized by the hUCMSCs was measured by an osteogenesis assay (mean ± sd; n = 5). Dissimilar letters at the bars indicate values that are significantly different ($p < 0.05$).